Journal of Magnetism and Magnetic Materials 446 (2018) 214–220

Contents lists available at ScienceDirect

Journal of Magnetism and Magnetic Materials

journal homepage: www.elsevier.com/locate/jmmm

Research articles

# Sulfur doping effect on microstructure and magnetic properties of Nd-Fe-B sintered magnets

Fang Yang [a], Yan-li Sui [b], Cun-guang Chen [a], Si-Yang Ye [b], Ping Li [a], Zhi-meng Guo [a,*], Vladislay Paley [c], Alex A. Volinsky [c,*]

[a] *Institute for Advanced Materials & Technology, University of Science and Technology Beijing, Beijing 100083, China*
[b] *State Key Laboratory for Advanced Metals and Materials, University of Science and Technology Beijing, Beijing 100083, China*
[c] *Department of Mechanical Engineering, University of South Florida, Tampa, FL 33620, USA*

ARTICLE INFO

*Article history:*
Received 26 May 2017
Received in revised form 8 August 2017
Accepted 8 September 2017
Available online 9 September 2017

*Keywords:*
Nd-Fe-B sintered magnets
Coercivity
S
Grain boundaries
Grain refinement

ABSTRACT

In this paper, the effects of sulfur (S) doping on microstructure and magnetic properties of Nd-Fe-B sintered magnets were studied. With 0.2 wt% S doping, the melting point of the Nd-rich eutectic phases decreased from 1038 K to 1021 K. Clear and continuous grain boundary phases were also formed with smaller grain size. The average grain size was 7.83 µm, which was approximately 1.3 µm smaller than that of the undoped magnets. The coercivity enhancement was attributed to boundary microstructure modification and grain size optimization. The coercivity of the 0.2 wt% S-doped magnets increased from 15.54 kOe to 16.67 kOe, with slight changes of the remanence and the maximum magnetic energy production. The magnetic properties of the overdoped magnets deteriorated, due to the reduction in density and decrease of the volume fraction of the main phase. Globular S precipitates in the Nd-rich triple junctions were hexagonal $Nd_2O_2S$ phase and tetragonal $NdS_2$ phase. S addition allows reducing Dy usage in magnets with comparable magnetic properties.

## 1. Introduction

Due to their high energy density, Nd-Fe-B sintered magnets have been applied in various fields [1,2]. However, the coercivity and the Curie temperature are too low for environmentally friendly applications in hybrid vehicles, electric vehicles, and wind power generators, where the required operating temperature is above 473 K [3–5]. At elevated temperatures, the effects of thermal activation on the reversal process are increased, which in turn decrease the coercivity [6,7]. Generally, partial substitution of Dy for Nd in the $Nd_2Fe_{14}B$ phase is effective to enhance the coercivity of Nd-Fe-B sintered magnets. $(Nd, Dy)_2Fe_{14}B$ has a higher magnetic anisotropy field, so Dy-containing magnets have higher coercivity when compared to Dy-free magnets [8]. However, there is a strong demand to reduce the usage of Dy from the highly coercive Nd-Fe-B sintered magnets because of high cost and the scarcity of the heavy rare earth elements. Furthermore, the heavy rare earth substitution leads to the decrease of produced energy [9,10]. Recently, many efforts have been undertaken to improve the coercivity of magnets without introducing Dy.

It is well known that coercivity is influenced not only by the magnetic anisotropy field of the $Nd_2Fe_{14}B$ phase, but also by the microstructure [11,12]. Coercivity can be enhanced by optimizing grain boundaries, lowering the melting temperature, and reducing the grain size [13–15]. According to previous work, the microstructure improvement can be achieved by the addition of non-rare earth elements. The grain growth inhibition can be achieved by the addition of Mo, W and Nb, due to the grain boundary pinning. The grain boundaries can be promoted with Al, Cu or Ga addition, because these elements reduce the melting point and improve wetting between the $Nd_2Fe_{14}B$ and Nd-rich phases [16–19]. Generally, sulfur (S) is thought to be an impurity element in most materials. Recently, demonstrations have shown that S powder addition is beneficial for coercivity enhancement [19–22]. Li et al. found that the coercivity of the $MoS_2$-added magnets was higher than the Mo-added magnets [20]. In the Dy/S co-doping magnets, S addition also produces a Dy-saving effect due to the suppressed formation of $(Nd, Dy)_xO_y$ phases in the triple junctions [21,22]. However, little information is available about the effects of S introduction on microstructure and magnetic properties of magnets, especially on melting point and grain size inhibition.

---

* Corresponding authors.
*E-mail addresses:* zmguo@ustb.edu.cn (Z.-m. Guo), volinsky@usf.edu (A.A. Volinsky).

https://doi.org/10.1016/j.jmmm.2017.09.023
0304-8853/

In this work, we investigated the effect of S doping in Nd-Fe-B sintered magnets with respect to the melting point, grain size, distribution of grain boundaries and magnetic properties. In addition, the distribution of S element was systematically studied and the mechanism of coercivity enhancement with S introduction in the magnets was established. We compared its magnetic and microstructural properties with those of the S-free magnets.

## 2. Experimental procedure

The commercial Nd-Fe-B and S powders were used as the raw materials. The purity of the raw materials was over 99%. Nd-Fe-B powders (~5 μm) with a nominal composition of 31.0Re(Re-Nd, Pr)-0.5Dy-bal.Fe-1.0B-4.0M(wt%, M-Cu, Al, Co, Cr), were mixed with various amounts of commercially available sulfur (0.0, 0.1, 0.2, 0.3, 0.5 wt%) powders. This was done by ball milling for 1 h using SPEX-8000 mixer/mill with steel balls and a ball-to-powder weight ratio was 5:1. The average particle size of S powder was about 5 μm. After being pressed by die-upset in a magnetic field of 17 kOe, the green compacts were vacuum-sintered at 1323 K for 3 h. Subsequently, the magnets were annealed at 1203 K for 3 h and subsequently annealed at 758 K for 6 h.

The magnets were cut into cylindrical shapes with a dimensional size of $\Phi\ 8 \times 5\ \text{mm}^3$ and mechanically polished. Density of the sintered magnets was determined by the Archimedes' principle measurement. The magnetic properties at room temperature of the processed magnets were measured by a magnetic measurement device (NIM-200C). Thermal analysis was performed using differential scanning calorimetry (DSC, NETZSCHSTA449) under protective Ar gas. Microstructural studies were conducted by field emission scanning electron microscope (FESEM, Supra55), operating at 15 kV. Average grain sizes and grain size distribution were evaluated by an image analyzer (UTHSCSA Image Tool). Phase composition and identification were performed using electron probe microanalysis (EPMA, JEOL, JXA-8230) and transmission electron microscopy (TEM, Tecnai G2 F30 S-TWIN) combined with energy dispersive spectroscopy detector (EDS, GENESIS) and selected area electron diffraction (SAED). The TEM analysis was carried out at 300 kV. In addition, thin foil specimens for the TEM analysis were prepared using an ion milling system.

## 3. Results and discussion

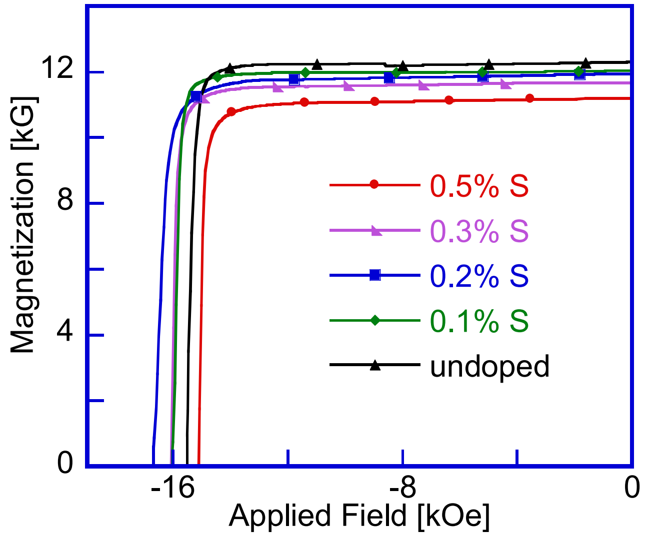

**Fig. 1.** Demagnetization curves for the undoped and S-doped magnets.

Table 1 and Fig. 1 show the corresponding magnetic performance for the S-free and S-doped magnets. The density of the undoped magnets is about 7.59 g/cm$^3$, while that of the 0.2 wt% S-doped magnets is 7.53 g/cm$^3$. When the S addition increased to 0.5 wt%, the density decreased to 7.42 g/cm$^3$. The density decreased with increasing S content, as summarized in Table 1. The measured coercivity $H_{cj}$, remanence $B_r$ and maximum magnetic energy product $(BH)_{max}$ values of the S-free magnets are 15.54 kOe, 12.30 kGs, and 36.71 MGsOe, respectively. With 0.1 wt% S addition, the $H_{cj}$ value increased to 16.03 kOe. When increasing the S content to 0.2 wt%, the coercivity reached its maximum value. The coercivity increased to 16.67 kOe, and the peak value was 7.3% higher than the S-free magnets. In addition, the Br decreased from 12.30 kGs to 11.95 kGs, and $(BH)_{max}$ changed from 36.71 MGsOe to 35.98 MGsOe. The introduction of S 0.2 wt% resulted in a slight decrease in $B_r$ and $(BH)_{max}$. Upon further increasing S content to 0.5 wt%, the magnetic performance of the magnets significantly decreased. The coercivity decreased from 16.67 kOe to 15.12 kOe. The proper S addition is beneficial to enhance the coercivity in the magnets. However, excessive S addition leads to the deterioration in magnet density and magnetic properties due to pores formation.

The microstructure changes and grain size distribution in the magnets with different S content are shown in Fig. 2. The dark gray regions are the $Nd_2Fe_{14}B$ main phases, and the bright regions correspond to the Nd-rich phases. The bright contrast of the grain boundaries suggests the existence of Nd-rich phases in the grain boundaries. The grain boundary phases (GBPs), in the undoped magnets, are discontinuous and not clearly visible, as seen in Fig. 2(a). This means that the Nd-rich phases are not connected well along the grain boundaries. In addition, the distribution of the main phase grains is not uniform. With S doping, grain boundaries of the magnets are changed in morphology, as seen in Fig. 2 (b) and (c). Compared to the S-free magnet, clearly visible and more continuous GBPs are observed in the 0.2 wt% S-doped magnets, isolating the $Nd_2Fe_{14}B$ grains. Thus, the surface defects at grain boundaries decreased, resulting in a suppression of the reversal domain nucleation at the GBPs which may deteriorate the coercivity. However, when increasing the S content to 0.5 wt%, there are many tiny defects along the grain boundaries, as seen in Fig. 2(c). Therefore, full densification cannot be easily achieved, as demonstrated by its low density of 7.42 g/cm$^3$.

In the undoped magnets, the average grain size is 9.14 μm which is relatively large, as seen in Fig. 2(d). In contrast, the grain

**Table 1**
Magnetic properties of the S-doped magnets as a function of the S content.

| Sample | Density [g·cm$^{-3}$] | $H_{cj}$ [kOe] | $B_r$ [kG] | $(BH)_{max}$ [MGsOe] | $H_k/H_{cj}$ |
|---|---|---|---|---|---|
| NdFeB | 7.59±0.01 | 15.54 | 12.30 | 36.71 | 0.97 |
| NdFeB + 0.1 wt%S | 7.58±0.01 | 16.03 | 12.03 | 36.24 | 0.97 |
| NdFeB + 0.2 wt%S | 7.53±0.01 | 16.67 | 11.95 | 35.98 | 0.96 |
| NdFeB + 0.3 wt%S | 7.47±0.01 | 16.07 | 11.67 | 35.06 | 0.96 |
| NdFeB + 0.5 wt%S | 7.42±0.01 | 15.12 | 11.19 | 33.88 | 0.94 |